Food Research International xxx (xxxx) xxx

Contents lists available at ScienceDirect

Food Research International

journal homepage: www.elsevier.com/locate/foodres

Hydrates of calcium citrate and their interconversion in relation to calcium bioaccessibility

Xiao-Chen Liu, Jacob J.K. Kirkensgaard, Leif H. Skibsted *

Department of Food Science, University of Copenhagen, Rolighedsvej 26, DK-1958 Frederiksberg C, Denmark

ARTICLE INFO

Keywords:
Calcium citrate
Dehydration
Dissolution
DSC
WAXS
DVS
Ostwald's stage law
Entropy-enthalpy compensation

ABSTRACT

Calcium citrate tetrahydrate (CCT) and hexahydrate (CCH) precipitates from aqueous solutions of $CaCl_2$ and sodium citrate above and below the transition temperature of 52 °C, respectively. The CCT, the dihydrate (CCD) and anhydrate (CCA) as obtained by a stepwise dehydration of solid CCH have enthalpy of dehydration of $\Delta H^0_{CCH\ to\ CCT} = 43.6$, $\Delta H^0_{CCT\ to\ CCD} = 43.8$, and $\Delta H^0_{CCD\ to\ CCA} = 88.1$ kJ·mol^{-1} as measured by DSC. WAXS measurements demonstrate a stepwise decrease in unit cell size upon dehydration, and a stronger binding of the two first water compared to additional. The increasing negative enthalpy of dissolution, as calculated from the temperature dependence of solubility (10–90 °C), +21 kJ·mol^{-1} (CCH), –20 kJ·mol^{-1} (CCT), –22 kJ·mol^{-1} (CCD), and –40 kJ·mol^{-1} (CCA) shows along the series of hydrates with increasing solubility, enthalpy–entropy compensation with an isoequilibrium temperature of 49 °C. Conversion of CCD and CCA in aqueous solutions yields the more soluble CCT, not the stable CCH in agreement with Ostwald's stage law, increasing calcium bioaccessibility under physiological conditions in intestines.

1. Introduction

Calcium is more bioavailable from calcium citrate than from more simple salts like calcium carbonate despite a common dissociation into calcium ions under gastric conditions of low pH (Pak, Harvey, & Hsu, 1987; Tondapu et al., 2009; Hanzlik, Fowler, & Fisher, 2005). Calcium citrate has even been found to promote bone growth under healing of bone fractures (Wang et al., 2012; Palermo et al., 2019). More recently a high bone mass and bone resorption has been found to correlate with high circulating citrate in adults (Hartley et al., 2020).

In the search for an explanation for these unique and somewhat unexpected properties of calcium citrate in relation to human nutrition and bone health, complex formation between calcium and citrate has been in focus (Holt, Lenton, Nylander, Sørensen, & Teixeira, 2014). Calcium binds to hydrogencitrate and even more strongly to citrate depending on pH (Vavrusova & Skibsted, 2016). Excess of citrate has thus been found to activate calcium from calcium citrate improving bioavailability (Sakhaee & Pak, 2013). However, complex formation alone does not fully explain these phenomena. The complex formation in the chyme under the neutral to alkaline conditions of the intestines, where calcium absorption occurs, competes with precipitation of calcium as phosphates, carbonates, phytates and palmitates (Goss, Lemons, Kerstetter, & Bogner, 2007). Moreover, both precipitation and complex formation will lower the free calcium concentration below the critical limit for absorption (Skibsted, 2016).

Calcium salts of hydroxycarboxylic acids like gluconic acid and citric acid spontaneously form supersaturated solutions in non-thermal processes, when calcium phosphates and other calcium salts of low solubility dissolves following addition of sodium hydroxycarboxylates (Skibsted, 2016). For certain combinations of hydroxycarboxylates spontaneous and robust supersaturation of up to a factor of 50 was observed with a lag phase for precipitation of days and even weeks (Vavrusova, Garcia, Danielsen, & Skibsted, 2017). Maybe the most surprising observation was the spontaneous supersaturation occurring, when calcium citrate tetrahydrate was dissolved in aqueous sodium citrate at a constant temperature (Vavrusova & Skibsted, 2016). Interaction between calcium citrate and citric acid/citrate is also seen as coupled diffusion under neutral to moderately acidic conditions, which also could be of importance for calcium bioavailability (Rodrigo, Ribeiro, Verissimo, Esteso, & Leaist, 2019).

Abbreviations: DSC, differential scanning calorimetry; DVS, dynamic vapor sorption; WAXS, wide-angle X-ray scattering; CCH, calcium citrate hexahydrate; CCT, calcium citrate tetrahydrate; CCD, calcium citrate dehydrate; CCA, anhydrous calcium citrate.

* Corresponding author.
E-mail addresses: xiaochen@food.ku.dk (X.-C. Liu), jjkk@food.ku.dk (J.J.K. Kirkensgaard), ls@food.ku.dk (L.H. Skibsted).

https://doi.org/10.1016/j.foodres.2020.109867
Received 6 August 2020; Received in revised form 23 October 2020; Accepted 28 October 2020
Available online 3 November 2020

Calcium citrate forms several well characterized hydrates, of which the tetrahydrate, when dissolved in aqueous solution, remains supersaturated with respect to precipitation of the more stable and less soluble hexahydrate (Vavrusova & Skibsted, 2016). This robust supersaturation also remains unexplained, but may relate to the spontaneous supersaturation observed, when sparingly soluble calcium hydroxycarboxylates dissolve in aqueous solution in the presence of other hydroxycarboxylates (Vavrusova et al., 2017). In order to obtain a better understanding for these supersaturation phenomena, clearly of importance for calcium metabolism and bone health, we have investigated the transformation between the hydrates of calcium citrate in the solid state and during equilibration with aqueous solutions, all within the framework of Ostwalds' stage law (Threlfall, 2003).

2. Materials and methods

2.1. Materials

Tricalcium dicitrate tetrahydrate ($Ca_3Citr_2{\cdot}4H_2O$, CCT, 99%), trisodium citrate dihydrate ($Na_3Citr{\cdot}2H_2O$), and Murexide were purchased from Sigma Aldrich (Steinheim, Germany). Calcium chloride dihydrate ($CaCl_2{\cdot}2H_2O$), ethylenediaminetetraacetic acid disodium salt dihydrate (EDTA), and sodium hydroxide (NaOH) were purchased from Merck (Darmstadt, Germany). The Milli-Q deionized water was made by Milli-Q Plus (Millipore Corp., Bedford, MA, USA).

2.2. Drying experiment

100 mg CCT and 100 mg calcium citrate hexahydrate ($Ca_3Citr_2{\cdot}6H_2O$, CCH) was dried in order to confirm the existence of calcium citrate dihydrate ($Ca_3Citr_2{\cdot}2H_2O$, CCD) and anhydrous (Ca_3Citr_2, CCA). CCT and CCH samples were dried stepwise in a drying cabinet with an increasing temperature from 75 °C to 110 °C and from 30 °C to 110 °C, respectively. All the samples were stored in air at 25 °C for three days after the drying process in the oven. All samples were weighed at different times in order to follow the mass changes during the whole drying and recovery process.

2.3. Synthesis

CCH was made by mixing an equal volume of Na_3Citr solution (0.030 M) and $CaCl_2$ solution (0.045 M) and after 24 h at room temperature, the precipitate was collected and washed with water followed by ethanol. By precipitation at 70 °C CCT was formed. The solid was dried at 25 °C in a drying cabinet for 3 days (Chattejee & Dhar, 1924). The CCD was made from CCT by drying at 80 °C for one week. The CCA was made from CCT by drying at 110 °C for one week.

2.4. Differential scanning calorimeter (DSC)

A total of about 10 mg of each sample was filled in 40 μL aluminum pan and the heat consumption during drying was determined by a DSC STAR^e System from Mettler Toledo (Schwerzenbach, Switzerland) with an empty aluminum pan as a reference (Cheng, Garcia, Tang, Danielsen, & Skibsted, 2018). The samples were measured from 25 °C to 200 °C with a scanning rate of 10 °C/min and the curves of heat flow over time was used to calculate the change of enthalpy (ΔH^0_{dehydr}) for the dehydration process of each salt using Eq. (1) (Mansour, 1994). H_F is the heat flow from DSC measurement, t is the time, m is the sample mass, and M is the molar mass (g/mol) of the sample.

$$\Delta H^0_{dehydr} = \int H_F dt/(m/M) \quad (1)$$

2.5. Determination of solubility product

EDTA titration was used for measuring the solubilities of CCH, CCT, CCD and CCA at different temperature of 10, 25, 37, 50, 70 and 90 °C. Suspension of each of the salts were prepared with 0.0015 mol salt and 100 mL Milli-Q water at investigated temperature. After equilibration the pH of solutions were measured by a pH meter (HQ411d; Hach Company, CO. USA), and the filtered solutions (Whatman paper, 42#; Whatman International Limited, Kent, UK) were titrated. A 0.002000 M EDTA solution and a 0.002000 M $CaCl_2$ solution were used as standards, and Murexide 0.5% was used as indicator (Harris, 2007). All the solutions with excess solid calcium citrate were equilibrated for half an hour with stirring in a baker in a thermostable water bath. Afterwards, the saturated solutions were filtered in an oven at the temperature of investigation. Then the total calcium concentrations of these saturated solutions were titrated by EDTA at room temperature.

The relationship between concentrations and activities of ions $X^{z\pm}$ is defined by:

$$a(X^{z\pm}) = \gamma^{z\pm}[X^{z\pm}] \quad (2)$$

where $a(X^{z\pm})$ is the activity of ion $X^{z\pm}$, and $[X^{z\pm}]$ is the concentration of ion $X^{z\pm}$. $\gamma^{z\pm}$ is the coefficient of activity of ion $X^{z\pm}$, which may be calculated by the expanded form of the Debye-Hückel equation:

$$log\gamma^{z\pm} = -A_{DH}z^2(\sqrt{I}/(1+\sqrt{I}) - 0.30I) \quad (3)$$

where A_{DH} is the Debye-Hückel constant with the values of 0.480, 0.510, 0.522, and 0.536 at 10, 25, 37, and 50 °C, respectively, and z is the charge of the ions. e.g. $z = 2$ for Ca^{2+} (Davies, 1962). I is the ionic strength of the aqueous solution as defined by

$$I = 0.5\sum(z^2[X^{z\pm}]) \quad (4)$$

Two chemical equilibria were considered, i.e. the precipitation equilibrium and the coordination equilibrium, for each solution based on activities:

$$Ca_3Citr_2{\cdot}xH_2O(s) \rightleftharpoons 3Ca^{2+} + 2Citr^{3-} + xH_2O \quad K_{sp,a} = (a(Ca^{2+}))^3 \cdot (a(Citr^{3-}))^2 \quad (5)$$

$$Ca^{2+} + Citr^{3-} \rightleftharpoons CaCitr^- \quad K_{ass,a} = a(CaCitr^-)/(a(Ca^{2+}) \cdot a(Citr^{3-})) \quad (6)$$

$K_{sp,a}$ is the solubility product based on the activities of the individual ions, and $K_{ass,a}$ is the association constant based on activities. The $K_{ass,a}$ values for $CaCitr^-$ are 5.04×10^4, 3.43×10^4, 3.84×10^4, 5.99×10^4 at 10, 25, 37, and 50 °C, respectively (Vavrusova & Skibsted, 2016), which when combined with the following for mass balance:

$$[Ca_{total}] = [Ca^{2+}] + [CaCitr^-] \quad (7)$$

and principle of electroneutrality:

$$2[Ca^{2+}] = 3[Citr^{3-}] + 2[HCitr^{2-}] + [H_2Citr^-] + [CaCitr^-] \quad (8)$$

allow for the calculation of calcium citrate speciation in aqueous solutions of calcium citrate also considering K_{a1}, K_{a2}, and K_{a3}, the dissociation constants of citric acid (Bates & Pinching, 1949):

$$H_3Citr \rightleftharpoons H^+ + H_2Citr^- \quad K_{a1} = a(H^+) \cdot a(H_2Citr^-)/a(H_3Citr) \quad (9)$$

$$H_2Citr^- \rightleftharpoons H^+ + HCitr^{2-} \quad K_{a2} = a(H^+) \cdot a(HCitr^{2-})/a(H_2Citr^-) \quad (10)$$

$$HCitr^{2-} \rightleftharpoons H^+ + Citr^{3-} \quad K_{a3} = a(H^+) \cdot a(Citr^{3-})/a(HCitr^{2-}) \quad (11)$$

Iterative methods were used in this type of calculation, in which I was given an initial value of 0.01. The concentrations of Ca^{2+}, $Citr^{3-}$, $CaCitr^-$, $HCitr^{2-}$, H_2Citr^-, and H_3Citr for each calcium citrate solution were calculated by combining the determined solubilities, measured pH, the given I, and solving Eqs. (2), (3) and (5)–(11) in each case. Afterward a new value of ionic strength I_{new} was calculated by combining ion

concentrations and Eq. (4). The iterative calculation continued until the value for ionic strength became constant as shown in Scheme S1.

For calculations of speciation at varying pH, the equilibrium

$$Ca^{2+} + HCitr^{2-} \rightleftharpoons CaHCitr \quad (12)$$

with $K_{ass,a} = 2600$ was also included in the iterative calculation (Vavrusova, Danielsen, Garcia, & Skibsted, 2018).

Using the concentrations and activities of each ion calculated from iterative calculation, the solubility products were calculated based on activities of calcium ions and citrate ions by Eq. (5). The solubility product based on concentration was calculated correcting all activities to concentrations using Eq. (3) for the actual ionic strength of the saturated calcium citrate solution at each temperature.

2.6. Determination of calcium ion activity

The activity of calcium ions in saturated solutions of the hydrates of calcium citrate and of the anhydrate was measured by a selective electrode ISE25Ca with a reference REF251 electrode from the Radiometer (Copenhagen, Denmark). The transition between the individual forms of calcium citrate were followed for up to 4 months at 25 °C. The standard for calibrating the electrode were calcium chloride solutions with concentrations of 1.00×10^{-4} M, 1.00×10^{-3} M, and 1.00×10^{-2} M. The calcium ion activities of the standard solutions were calculated by Eq. (2) (Cheng et al., 2018).

2.7. Dynamic vapor sorption (DVS)

A total of about 10 mg for each of the hydrates of calcium citrate and for the anhydrous calcium citrate was used for establishment of sorption isotherms and hysteresis curves. The curves were measured by DVS 1 system (Surface Measurements System, London, UK) with an equilibration sorption criterion of 0.002%/min at 25 °C (Hagelstein, Gerhart, & Wagner, 2018).

2.8. Wide-angle X-ray scattering (WAXS)

WAXS is a technique for analyzing the structure of particle systems in terms of averaged sizes or shapes. WAXS profiles were measured using a GANESHA instrument from SAXSLAB (Lyngby, Denmark). The instrument uses a Rigaku (Rigaku-Denki, Co., Tokyo, Japan) 40 W microfocused Cu-source producing X-rays with a wavelength of $\lambda = 1.54$ Å detected by a moveable Pilatus 300 k pixel-detector from Dectris (Baden, Switzerland) allowing different length scales to be measured. The two-dimensional scattering data were azimuthally averaged and corrected for detector inhomogeneities using standard reduction software (SAXSGUI). The radially averaged intensity (*Int.*) is given as a function of the scattering vector $q = 4\pi \cdot \sin\theta/\lambda$, where λ is the wavelength and 2θ is the scattering angle. For the WAXS this covers a q-range from 0.23 to 3.1 Å corresponding to an upper 2θ value of 44.6° or 2.03 Å.

3. Results

Three hydrates of calcium citrate are well-characterized, the hexahydrate (CCH), the tetrahydrate (CCT), and the dihydrate (CCD) together with anhydrous calcium citrate (CCA). CCH and CCT are obtained by precipitation from aqueous solutions of calcium chloride and sodium citrate below and above the transition temperature of 52 °C, respectively (Chattejee & Dhar, 1924). The CCH was the common polymorphic form and not the form as is known from hydrothermal synthesis at lower temperature. This should be evident from the WAXS pattern as seen in Fig. 3 compared to the diffraction pattern recently published (Kaduk, 2018). CCD and CCA are obtained by drying of the higher hydrates. As

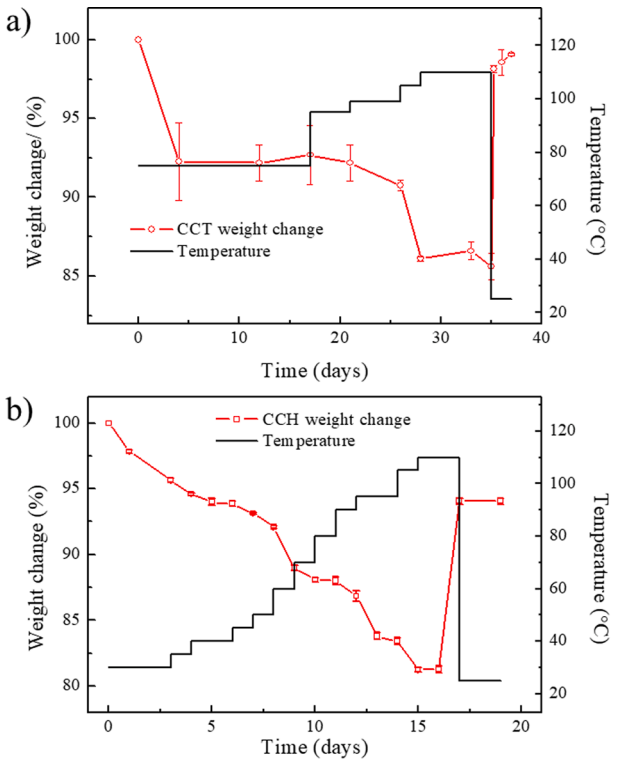

Fig. 1. Thermogravimetric analysis for hexahydrate (CCH, a) and tetrahydrate (CCT, b) of calcium citrate. Mass changes of 2.97 % and 3.16 % for CCH and CCT, respectively, correspond to loss of one molecule of water for each molecule of calcium citrate.

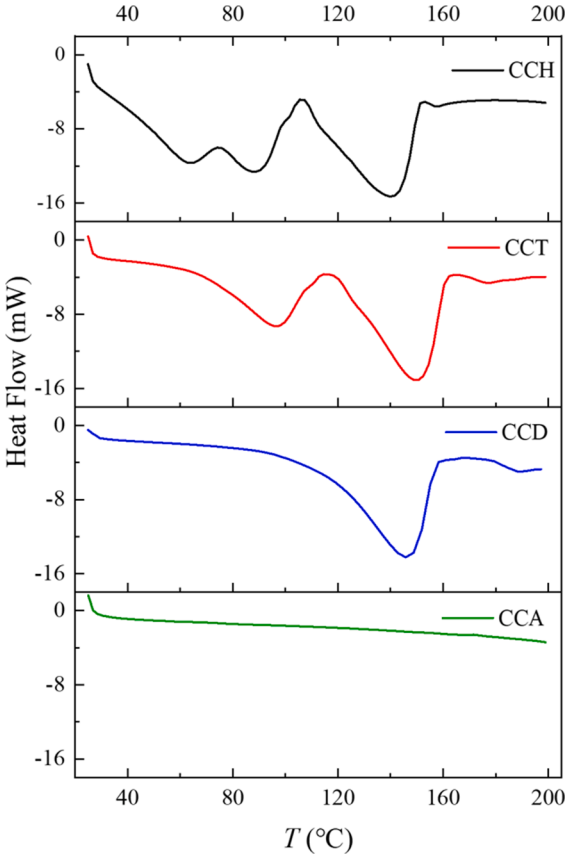

Fig. 2. DSC curves of hexahydrate (CCH), tetrahydrate (CCT), dihydrate (CCD), and anhydrate (CCA) of calcium citrate.

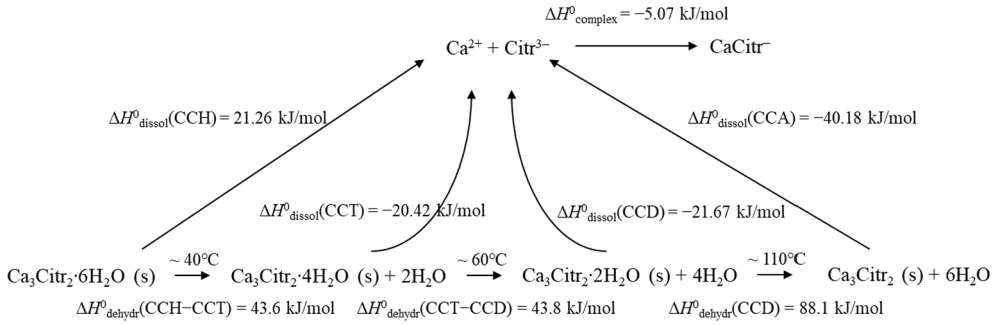

Scheme 1. Dehydration and dissolution processes of CCH, CCT, CCD and CCA. Dissolution enthalpies (ΔH^0_{dissol}) are from the solubility products at different temperatures (Fig. 5). Dehydration enthalpies (ΔH^0_{dehydr}) are obtained from integrations of DSC curves (Fig. 2) according to Eq. (1). $\Delta H^0_{complex}$ is from Vavrusova and Skibsted (2016).

seen in Fig. 1a, the weight loss of ~7.5% for CCT corresponds to two water molecules for drying stepwise up to 95 °C, while the weight loss of ~13.9% corresponds to four water molecules for drying up to 110 °C. The dried CCT products are CCD and CCA in the temperature regions of 75–95 °C and 105–110 °C, respectively, as confirmed by DSC measurements. Both CCD and CCA absorb vapor from air, and CCT but not CCH is formed according to the mass change, and to the DSC thermograms of the dried CCD and CCA equilibrated in air. CCH drying experiments showed similar results as shown in Fig. 1b, and CCH dried to form CCT, CCD, and CCA at 40 °C, 80 °C, and 110 °C, respectively.

DSC thermograms of CCT and CCH, and of CCD and CCA obtained by drying CCT are shown in Fig. 2. The thermograms show three endothermic events for CCH positioned at 63, 88, and 140 °C. For CCT two endothermic events are recognized at 96 and 151 °C, while for CCD only one endothermic event at 146 °C is recognized. CCA shows no indication

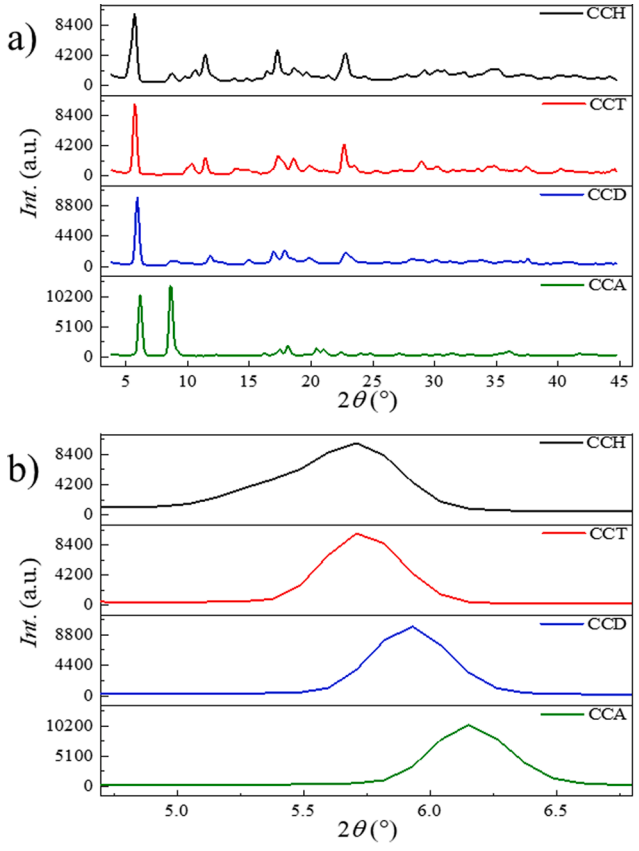

Fig. 3. The intensity (*Int.*) against 2θ curves for hexahydrate, tetrahydrate, dihydrate, and anhydrate of calcium citrate from WAXS.

Table 1
Solubility of hexahydrate (CCH), tetrahydrate (CCT), dihydrate (CCD) and anhydrous calcium citrate (CCA) in water as determined by EDTA titration.[a]

Temp./°C	CCH/mM	CCT/mM	CCD/mM	CCA/mM
10	2.449 ± 0.029	5.436 ± 0.041	5.485 ± 0.030	8.848 ± 0.061
25	3.141 ± 0.029	4.646 ± 0.068	4.939 ± 0.030	7.045 ± 0.015
37	3.746 ± 0.058	4.360 ± 0.054	4.242 ± 0.030	5.788 ± 0.030
50	3.904 ± 0.014	4.101 ± 0.068	4.061 ± 0.061	4.621 ± 0.136
70	3.947 ± 0.029	3.460 ± 0.027	3.788 ± 0.030	4.045 ± 0.015
90	4.250 ± 0.014	2.772 ± 0.020	3.076 ± 0.015	3.258 ± 0.045

[a] Solubility was based on concentration of total calcium.

of endothermic events. The endothermic event at 63 °C is accordingly assigned to loss of two water from CCH to form CCT, while the endothermic event at 89 °C is assigned to loss of two additional water to form CCD, and the endothermic event at 141 °C is assigned to the loss of the final two water molecules to form CCA at 150 °C. The last two transformations are also seen in the thermograms of CCT now at 96 °C and 151 °C, respectively, and the high temperature transformation in the thermogram for CCD is seen at 146 °C. The enthalpies of dehydration as calculated from the integrated area based on Eq. (1) for CCH are 77.7 kJ/mol from 43.1 °C to 106.1 °C, and 97.8 kJ/mol from 106.1 °C to 152.5 °C, respectively. For CCT the enthalpies of dehydration are 45.1 kJ/mol from 62.4 °C to 115.5 °C, and 86.8 kJ/mol from 115.5 °C to 165.0 °C, respectively. For CCD the enthalpy of dehydration is 88.1 kJ/mol from 92.5 °C to 162.0 °C. The dehydration enthalpy (ΔH^0_{dehydr}) of CCH, CCT, and CCD as calculated by Eq. (1) are shown in Scheme 1. The values of ΔH^0_{dehydr} for losing two crystal waters follows the order CCH ≈ CCT ≫ CCD. The reported values are from dehydration using a heating rate of 10 K·min^{-1}. Heating rate was varied between 1 K·min^{-1} and 15 K·min^{-1}, and heating rate did not influence the enthalpy of dehydration but the

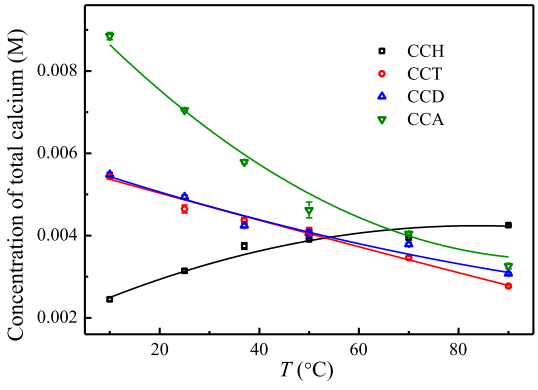

Fig. 4. The solubilities of hexahydrate (CCH), tetrahydrate (CCT), dihydrate (CCD), and anhydrate (CCA) of calcium citrate based on the total calcium concentration at different temperatures.

Table 2
Ion speciation in homogeneous saturated solutions of hexahydrate (CCH), tetrahydrate (CCT), dihydrate (CCD) and anhydrous calcium citrate (CCA) in water, and solubility product based on concentrations and on activities.

Citrate type	Temp. (°C)	pH	Concentration of the main species (M)						Activity of the main species					$K_{sp,c}$ /M^5	$K_{sp,a}$
			[Ca^{2+}]	[$Citr^{3-}$]	[$CaCitr^-$]	[$HCitr^{2-}$]	[H_2Citr^-]	[H_3Citr]	a(Ca^{2+})	a($Citr^{3-}$)	a($CaCitr^-$)	a($HCitr^{2-}$)	a(H_2Citr^-)	Ca_3Citr_2	
CCH	**10**	6.05	9.84×10^{-4}	6.18×10^{-5}	1.47×10^{-3}	1.02×10^{-4}	4.34×10^{-6}	4.90×10^{-9}	7.69×10^{-4}	3.55×10^{-5}	1.38×10^{-3}	7.95×10^{-5}	4.08×10^{-6}	3.65×10^{-18}	5.75×10^{-19}
	25	6.22	1.26×10^{-3}	1.00×10^{-4}	1.88×10^{-3}	1.07×10^{-4}	3.02×10^{-6}	2.29×10^{-9}	9.53×10^{-4}	5.37×10^{-5}	1.76×10^{-3}	8.13×10^{-5}	2.82×10^{-6}	2.00×10^{-17}	2.50×10^{-18}
	37	6.25	1.45×10^{-3}	9.99×10^{-5}	2.30×10^{-3}	9.76×10^{-5}	2.53×10^{-6}	1.78×10^{-9}	1.08×10^{-3}	5.15×10^{-5}	2.13×10^{-3}	7.27×10^{-5}	2.35×10^{-6}	3.04×10^{-17}	3.33×10^{-18}
	50	6.46	1.41×10^{-3}	6.98×10^{-5}	2.49×10^{-3}	4.24×10^{-5}	6.82×10^{-7}	2.97×10^{-10}	1.06×10^{-3}	3.65×10^{-5}	2.32×10^{-3}	3.18×10^{-5}	6.34×10^{-7}	1.38×10^{-17}	1.59×10^{-18}
CCT	**10**	5.87	2.11×10^{-3}	8.84×10^{-5}	3.33×10^{-3}	1.94×10^{-4}	1.17×10^{-5}	1.94×10^{-8}	1.49×10^{-3}	4.06×10^{-5}	3.05×10^{-3}	1.38×10^{-4}	1.07×10^{-5}	7.30×10^{-17}	5.48×10^{-18}
	25	6.00	1.87×10^{-3}	1.17×10^{-4}	2.78×10^{-3}	1.94×10^{-4}	8.71×10^{-6}	1.08×10^{-8}	1.34×10^{-3}	5.55×10^{-5}	2.56×10^{-3}	1.39×10^{-4}	8.02×10^{-6}	8.89×10^{-17}	7.46×10^{-18}
	37	5.84	1.80×10^{-3}	9.77×10^{-5}	2.56×10^{-3}	2.36×10^{-4}	1.54×10^{-5}	2.77×10^{-8}	1.30×10^{-3}	4.71×10^{-5}	2.36×10^{-3}	1.71×10^{-4}	1.42×10^{-5}	5.60×10^{-17}	4.91×10^{-18}
	50	5.94	1.57×10^{-3}	6.66×10^{-5}	2.53×10^{-3}	1.32×10^{-4}	6.93×10^{-6}	9.95×10^{-9}	1.16×10^{-3}	3.37×10^{-5}	2.34×10^{-3}	9.72×10^{-5}	6.42×10^{-6}	1.72×10^{-17}	1.78×10^{-18}
CCD	**10**	5.62	2.26×10^{-3}	8.23×10^{-5}	3.22×10^{-3}	3.18×10^{-4}	3.36×10^{-5}	9.94×10^{-8}	1.58×10^{-3}	3.69×10^{-5}	2.95×10^{-3}	2.23×10^{-4}	3.07×10^{-5}	7.85×10^{-17}	5.42×10^{-18}
	25	5.76	2.10×10^{-3}	1.12×10^{-4}	2.84×10^{-3}	3.16×10^{-4}	2.44×10^{-5}	5.24×10^{-8}	1.48×10^{-3}	5.12×10^{-5}	2.60×10^{-3}	2.23×10^{-4}	2.23×10^{-5}	1.16×10^{-16}	8.54×10^{-18}
	37	5.97	1.71×10^{-3}	1.00×10^{-4}	2.54×10^{-3}	1.81×10^{-4}	8.83×10^{-6}	1.18×10^{-8}	1.24×10^{-3}	4.91×10^{-5}	2.34×10^{-3}	1.32×10^{-4}	8.15×10^{-6}	4.97×10^{-17}	4.63×10^{-18}
	50	5.90	1.57×10^{-3}	6.56×10^{-5}	2.49×10^{-3}	1.42×10^{-4}	8.21×10^{-6}	1.29×10^{-8}	1.16×10^{-3}	3.32×10^{-5}	2.31×10^{-3}	1.05×10^{-4}	7.62×10^{-6}	1.67×10^{-17}	1.73×10^{-18}
CCA	**10**	5.72	3.41×10^{-3}	1.13×10^{-4}	5.44×10^{-3}	3.19×10^{-4}	2.54×10^{-5}	5.88×10^{-8}	2.23×10^{-3}	4.36×10^{-5}	4.89×10^{-3}	2.09×10^{-4}	2.29×10^{-5}	5.09×10^{-16}	2.10×10^{-17}
	25	5.71	2.93×10^{-3}	1.37×10^{-4}	4.12×10^{-3}	4.06×10^{-4}	3.37×10^{-5}	8.02×10^{-8}	1.96×10^{-3}	5.55×10^{-5}	3.73×10^{-3}	2.72×10^{-4}	3.05×10^{-5}	4.68×10^{-16}	2.31×10^{-17}
	37	5.69	2.42×10^{-3}	1.09×10^{-4}	3.36×10^{-3}	3.53×10^{-4}	3.15×10^{-5}	7.91×10^{-8}	1.68×10^{-3}	4.77×10^{-5}	3.07×10^{-3}	2.44×10^{-4}	2.87×10^{-5}	1.70×10^{-16}	1.07×10^{-17}
	50	5.61	1.90×10^{-3}	6.43×10^{-5}	2.72×10^{-3}	2.63×10^{-4}	2.90×10^{-5}	8.85×10^{-8}	1.37×10^{-3}	3.07×10^{-5}	2.51×10^{-3}	1.89×10^{-4}	2.67×10^{-5}	2.84×10^{-17}	2.40×10^{-18}

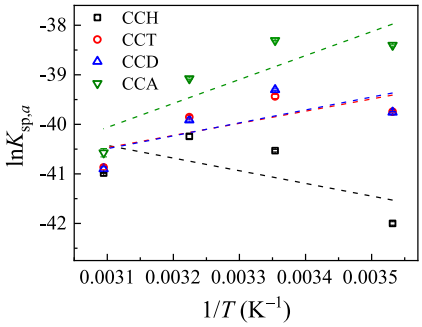

Fig. 5. The temperature effects on the solubility products of hexahydrate (CCH), tetrahydrate (CCT), dihydrate (CCD), and anhydrate (CCA) of calcium citrate in water based on the activities of Ca^{2+} and $Citr^{3-}$. The enthalpies of dissolution ΔH^0_{dissol} are presented in Table 4b.

temperature of the dehydration increased for increasing scanning rate.

The crystal structures of the three hydrates and the anhydrous form of calcium citrate were different as shown by WAXS measurements in the q range of 0.23–3.1 Å. The *Int./2θ* curves of citrates with crystal waters, CCH, CCT, and CCD had similar peak shapes for the scattering with the CCA being more different compared to others, as seen in Fig. 3a. The *Int./2θ* curves of CCH, CCT, and CCA corresponded to the XRD previously reported as shown in Fig. S1 (Kaduk, 2018). The crystal peak around $2\theta = 5.7°$ have a right shift increasing with the decreasing amount of crystal water in agreement with a tighter structure upon loss of crystal water, see Fig. 3b.

The solubilities of the different types of calcium citrates were measured at different temperatures from 10 to 90 °C by a titration method, see Table 1. In a comparison with CCT, the solubilities of CCD are marginally higher, the CCA are considerably higher up to 50 °C. The solubilities of these three forms of calcium citrate have a similar trend decreasing for increasing temperature. The solubility of CCH was found lower than for CCT up to approximately 51 °C. Above this temperature the solubility of CCH became higher than the solubility of CCT and CCD, and continued to increase, as shown in Fig. 4.

The solubilities are shown in Table 1 as total calcium concentrations which was used to calculate the concentrations and activities of the main ion species present in the solutions together with the solubility products using combinations of Eqs. (2)–(11) at 10–50 °C, see Table 2, using the iteration procedure as shown in Scheme S1. The solubility products based on activities were used to calculate the dissolution enthalpy (ΔH^0_{dissol}) for CCH, CCT, CCD and CCA according to Eq. (13), see Fig. 5. The ΔH^0_{dissol} was found to have the value 21.26 kJ/mol for CCH, –20.42 kJ/mol for CCT, −21.67 kJ/mol for CCD, and −40.18 kJ/mol for CCA as shown in Scheme 1.

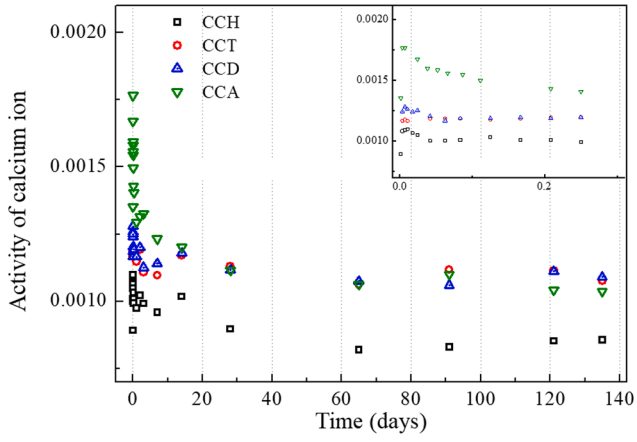

Fig. 6. Calcium ion activity during 4 months in saturated calcium citrate solutions of hexahydrate (CCH), tetrahydrate (CCT), dihydrate (CCD), and anhydrate (CCA). Insert is the magnification of the initial period.

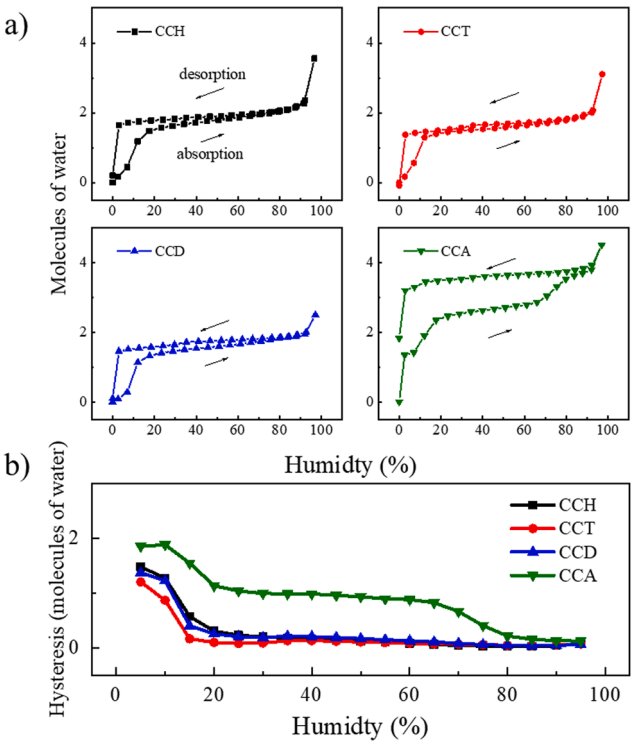

Fig. 7. Water sorption isotherms and hysteresis curves for hydrates of calcium citrate and for the anhydrate.

$$lnK_{sp} = -\Delta H^0_{dissol}/R \cdot 1/T + \Delta S^0_{dissol}/R \quad (13)$$

According to the values of ΔH^0_{dehydr} and ΔH^0_{dissol} shown in Scheme 1, for the four solid calcium citrate salts, the CCH transformation to CCT occurs at around 40 °C, while CCT transforms to CCD and CCA by drying at 60 and 110 °C, respectively. CCD and CCA could recover to CCT by absorbing vapor from air at temperatures below 40 °C.

Among the saturated aqueous solutions of calcium citrate, transition between the hydrates was also demonstrated. Fig. 6 shows the changes in calcium ion activity ($a(Ca^{2+})$) of saturated calcium citrate solutions with time in water at 25 °C. The $a(Ca^{2+})$ of CCT and CCH were very stable after stirring for several hours, but the $a(Ca^{2+})$ of CCD and CCA kept decreasing until the same activity as was found for a saturated solutions of CCT, indicating the transition from CCD and CCA and to CCT, but not further to the thermodynamically most stable form, CCH.

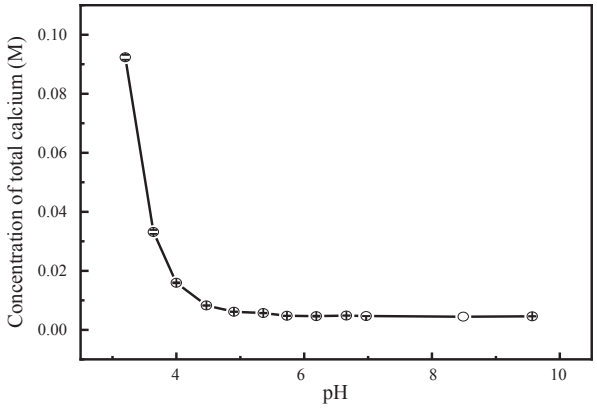

Fig. 8. Total calcium concentration in saturated solutions of calcium citrate tetrahydrate of varying pH at 25 °C.

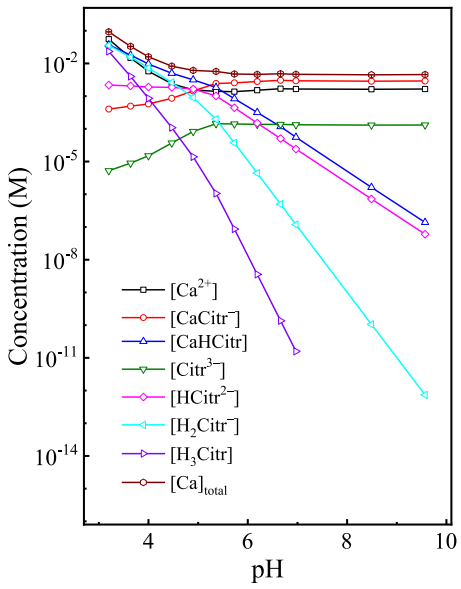

Fig. 9. Speciation in saturated solution of calcium citrate tetrahydrate at 25 °C at indicated pH. The speciation at varying pH are presented in Table 3.

The calcium activity in the saturated solutions of CCT and CCH stayed constants for up to four months without any transformations in saturated aqueous solutions.

In agreement with the apparent inertness of CCT compared both to CCA and CCD and compared to CCH, the sorption isotherm for CCT showed less hysteresis than the sorption isotherm of CCA, CCD and CCH, see Fig. 7.

The unique properties of CCT was investigated further in relation to the pH dependence of the solubility and a possible pH-dependent transformation of the less stable but inert CCT to the stable CCH at 25 °C. The pH effect on solubility of calcium were investigated for saturated CCT aqueous solutions, and solubility became lower with increasing pH, see Fig. 8. The dominating calcium speciation at lower pH, are Ca^{2+} and CaHCitr. The $CaCitr^-$ is the main soluble calcium for pH higher than ~5.5 as shown in Fig. 9 and Table 3. The robustness of supersaturated solutions of calcium citrate at "natural" pH of these solutions (Table 2) may accordingly be assigned to the slow precipitation reaction:

$$Ca^{2+} + 2CaCitr^- + 4H_2O \rightleftharpoons Ca_3Citr_2{\cdot}4H_2O \quad (14)$$

Under the slightly alkaline conditions of the intestines calcium citrate dissolved at the lower pH of the stomach may stay in solution and if precipitated form the tetrahydrate. Both the higher solubility of CCT and the robustness of supersaturated CCT solutions seems to contribute to the higher bioaccessibility of calcium citrate compared to other calcium salts.

Upon acidification of solutions of calcium citrate hydrates, $HCitr^{2-}$ will form, and especially around pH of 5 induce precipitation of the hexahydrate with its lower solubility, see Table 2 for solubility products. Accordingly, for a pH region just below neutrality, calcium citrate may precipitate and decrease in equilibrium solubility, see Fig. 9 and Table 3.

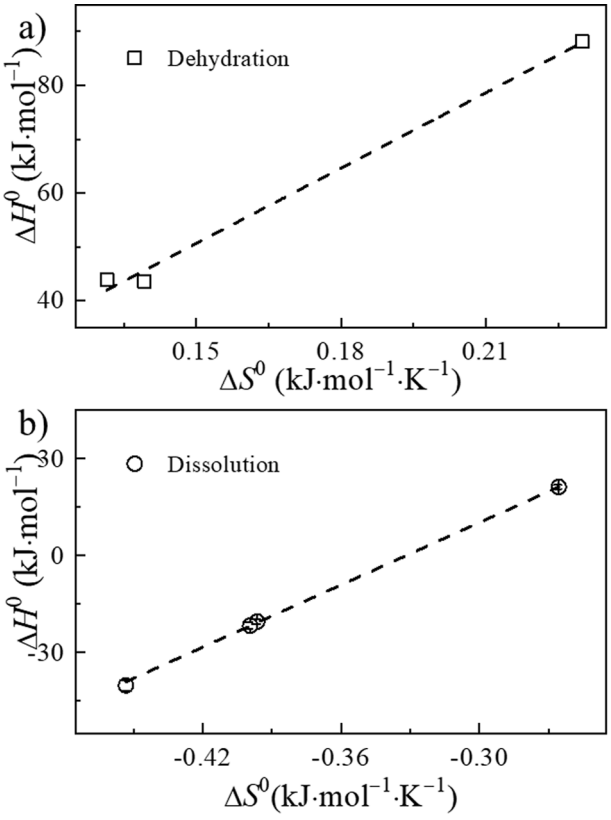

Fig. 10. Enthalpy-entropy compensation for dehydration (a) and dissolution (b) $\Delta H^0_{dehydr} = ((193.7 + 273.2) \pm 35.0)\ \Delta S^0_{dehydr} - (19.4 \pm 6.0)$ ($R^2 > 0.98$); and $\Delta H^0_{dissol} = ((48.6 + 273.2) \pm 6.1)\ \Delta S^0 + (106.8 \pm 2.1)$.) ($R^2 > 0.99$). The detailed values are shown in Table 4.

4. Discussion

Calcium citrate represent an interesting example of a salt, where the dehydration enthalpy for a series of hydrates correlates with the heat of dissolution of the same salts. The decreasing solubility along the series CCA > CCD > CCT > CCH at 25 °C indicates that CCA has a higher aqueous solubility than the hydrated form of calcium citrate. Crystal structures are available and the vacancies in the crystals of the less hydrated calcium citrates lead to holes inducing a structure collapse and smaller crystal cell as show in Fig. 3 (Kaduk, 2018). The property of CCA is quite different compared to the hydrates due to absence of crystal water (Herdtweck, Kornprobst, Sieber, Straver, & Plank, 2011). The two crystal waters of CCD are coordinated strongly to calcium and are difficult to remove. The structures and properties of CCD and CCT are similar and the dominance of the two strongly coordinated waters entails similar reverse solubilities, water sorption behaviors and crystal structures for CCD and CCT.

The transition processes among the hydrates and anhydrate of calcium citrate were investigated for each of the salts in saturated aqueous

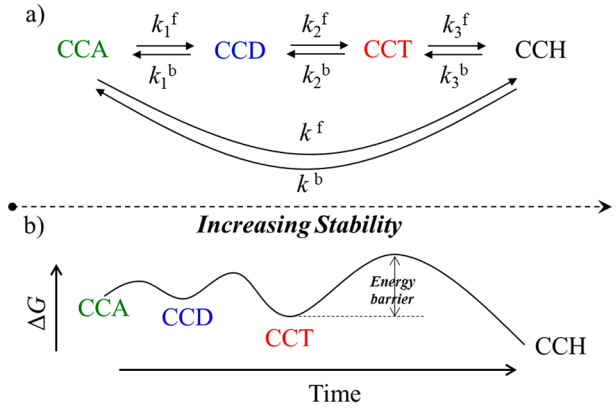

Scheme 2. (a) Transition between anhydrous calcium citrate and calcium citrate hydrates in saturated aqueous solutions at 25 °C: rate constants for forward reaction (k^f) and backward process (k^b); (b) The transition process among the four types of calcium citrate depicted according to the Ostwald's stage law.

Table 3
Speciations of saturated aqueous calcium citrate tetrahydrate solutions at 25 °C of different pH based on total calcium as determined by EDTA titration and iterative calculations.

pH	$[Ca^{2+}]$	$[CaCitr^{-}]$	[CaHCitr]	$[Citr^{3-}]$	$[HCitr^{2-}]$	$[H_2Citr^{-}]$	$[H_3Citr]$	$[Ca]_{total}$
3.20	5.49×10^{-2}	4.03×10^{-4}	3.70×10^{-2}	5.24×10^{-6}	2.19×10^{-3}	3.57×10^{-2}	2.33×10^{-2}	9.24×10^{-2}
3.64	1.47×10^{-2}	4.96×10^{-4}	1.80×10^{-2}	8.96×10^{-6}	2.05×10^{-3}	1.56×10^{-2}	4.00×10^{-3}	3.32×10^{-2}
4.00	5.78×10^{-3}	5.78×10^{-4}	9.59×10^{-3}	1.50×10^{-5}	1.91×10^{-3}	7.28×10^{-3}	8.56×10^{-4}	1.59×10^{-2}
4.47	2.40×10^{-3}	8.61×10^{-4}	5.00×10^{-3}	3.69×10^{-5}	1.86×10^{-3}	2.64×10^{-3}	1.09×10^{-4}	8.26×10^{-3}
4.90	1.55×10^{-3}	1.44×10^{-3}	3.15×10^{-3}	8.32×10^{-5}	1.65×10^{-3}	9.03×10^{-4}	1.40×10^{-5}	6.14×10^{-3}
5.36	1.40×10^{-3}	2.43×10^{-3}	1.85×10^{-3}	1.44×10^{-4}	1.02×10^{-3}	1.97×10^{-4}	1.06×10^{-6}	5.69×10^{-3}
5.73	1.37×10^{-3}	2.55×10^{-3}	8.36×10^{-4}	1.41×10^{-4}	4.42×10^{-4}	3.74×10^{-5}	8.67×10^{-8}	4.76×10^{-3}
6.19	1.52×10^{-3}	2.83×10^{-3}	3.18×10^{-4}	1.37×10^{-4}	1.50×10^{-4}	4.42×10^{-6}	3.56×10^{-9}	4.63×10^{-3}
6.66	1.69×10^{-3}	3.04×10^{-3}	1.17×10^{-4}	1.37×10^{-4}	5.05×10^{-5}	5.01×10^{-7}	1.36×10^{-10}	4.85×10^{-3}
6.97	1.66×10^{-3}	2.95×10^{-3}	5.56×10^{-5}	1.33×10^{-4}	2.42×10^{-5}	1.18×10^{-7}	1.58×10^{-11}	4.66×10^{-3}
8.49	1.63×10^{-3}	2.86×10^{-3}	1.63×10^{-6}	1.30×10^{-4}	7.18×10^{-7}	1.06×10^{-10}	0	4.49×10^{-3}
9.57	1.66×10^{-3}	2.92×10^{-3}	1.38×10^{-7}	1.31×10^{-4}	6.00×10^{-8}	7.36×10^{-13}	0	4.57×10^{-3}

solutions by measurement of calcium ion activity and for the solid compounds by DSC measurements. The CCA and CCD transform to CCT in a few days in contact with water, but the CCT is not transformed further to CCH despite a negative ΔG for this process. As shown in Scheme 1 ΔH^0_{dissol} of CCT is negative compared to ΔH^0_{dissol} of CCH which is positive. According to Ostwald's stage law, the transformation along a series of hydrates with increasing numbers of crystal water is an enthalpy decreasing process, and the transformation order should be CCA → CCD → CCT → CCH (Van Santen, 1984; Casey, 1988). However, the energy barrier increases and the transformation rate decreases for transformation to the increasingly more stable form, see Scheme 2b (Schmelzer & Abyzov, 2017; Chung, Kim, Kim, & Kim, 2009). The precipitates of both of CCT and CCH can coexist in equilibrium in aqueous solutions. The Ca^{2+} activity of a saturated solution of CCT did not decrease and DSC thermograms of CCT isolated from the saturated solution remained unchanged for at least 4 months as shown in Figs. 6 and S3. The transition between CCT and CCH in equilibrium with dissolved calcium citrate in water includes at least two steps CCT solid → aqueous solution → CCH solid. However, CCH appears from CCT following adjustment of pH to lower values indicating that the rate determining step must be the dissolution of CCT while the step in which CCH precipitates from solution must be fast. Hence the process CCT solid → aqueous solution is the rate controlling step in effect making the CCT dominating for a long time in pseudo equilibrium with the aqueous solution. Newly formed CCH precipitated on the surface of CCT may also hamper dissolution of CCT.

The solubility of CCT is higher than CCH at room temperature and while CCH is the stable form, CCT is inert in a pseudo equilibrium with the aqueous solutions. CCT has accordingly been the first choice for beverage or food supplements, and patents have protected synthesis methods in which CCT are made from boiling solutions of $CaCl_2$ and Na_3Citr or other combination of calcium and citrate salts. (Chattejee & Dhar, 1924; Bailey, Nehmer, & Elmore, 2010) The CCH can be produced by mixing the solutions of $CaCl_2$ and Na_3Citr at room temperature (Chattejee & Dhar, 1924), in agreement with the solubility curves for calcium citrate hydrates as seen in Fig. 4. The CCT have higher solubility than the CCH increasing the bioaccessibility of calcium from the intestines at physiological temperature.

Table 4
Enthalpies of dehydration (a) and dissolution (b) of calcium citrates from Scheme 1. Entropies for dehydration were calculated at equilibrium temperature from enthalpies of dehydration using Eq. (15). Enthalpies for dissolution were calculated from solubility product at varying temperature using Eq. (13), and isoequilibrium entropies for dissolution were calculated according to Eq. (16).

(a)

Dehydration	ΔH^0/kJ·mol^{-1}	ΔS^0/kJ·mol^{-1}·K^{-1}
CCH to CCT	43.6	0.139
CCT to CCD	43.8	0.131
CCD to CCA	88.1	0.230

(b)

Dissolution	ΔH^0/kJ·mol^{-1}	ΔS^0/kJ·mol^{-1}·K^{-1}
CCH	21.26 ± 0.64	−0.266 ± 0.002
CCT	−20.42 ± 0.76	−0.396 ± 0.003
CCD	−21.67 ± 1.04	−0.399 ± 0.004
CCA	−40.18 ± 1.66	−0.453 ± 0.006

For dehydration the equilibrium temperatures as determined by DSC are shown in Table 4 and for these conditions the ΔS^0_{dehydr} may be calculated from:

$$\Delta S^0_{dehydr} = \Delta H^0_{dehydr}/T_{trans}, \text{ for } \Delta G^0_{dehydr} = 0 \quad (15)$$

the enthalpy–entropy compensation (Dutronc et al., 2013; Griessen et al., 2020) seen in Fig. 10a with an isoequilibrium temperature of 193 °C confirms the homologue transfer along the hydrates of the calcium citrate. This is further confirmed for the thermodynamics of the dissolution of the calcium citrates for which:

$$\Delta H^0_{dissol} = T_{isoeq}\Delta S^0 + \text{constant} \quad (16)$$

provides an isoequilibrium temperature of 49 °C very close to the temperature for which the hydrates of calcium citrates have the same solubility, see Fig. 10b.

The enthalpy–entropy compensation demonstrated for calcium citrates may be most important for the dissolution of calcium citrate hydrates. The unique dissolution behavior of calcium citrate hydrates with one hydrate dissolution (CCH) being endothermic, while the others being exothermic (CCT, CCD, CCA), seems to explain the robustness of supersaturated solutions of calcium citrates. The dissolution enthalpy covering a range of more than 60 kJ·mol^{-1} along the series (−)CCA < CCD < CCT < CCH(+) is perfectly compensated by a decreasing negative entropy of dissolution along the same series CCA < CCD < CCT < CCH with an isoequilibrium temperature of 49 °C, in effect leaving the solubility comparable around physiological temperature for both endothermic and exothermic dissolution processes.

5. Conclusion

The hydrate of calcium citrate with the highest enthalpy of dehydration has the most negative enthalpy of dissolution and the most significant hysteresis for dehydration-hydration cycles as measured by DVS. Both solid anhydrous and solid dihydrate calcium citrate in equilibrium with a saturated aqueous solution at 25 °C convert in a few days to a saturated solution of the tetrahydrate without further conversion to the more stable and less soluble hexahydrate. The metastability of the tetrahydrate at physiological temperature, and neutral to alkaline conditions, in effect increasing solubility as a consequence of Ostwalds stage law, seems to increase bioaccessibility of calcium from calcium citrate in intestines. In contrast, moderate acidification and readjustment of pH induce conversion to the stable hexahydrate pointing towards a role of

the CaHCitr complex in this transformation under gastric conditions.

CRediT authorship contribution statement

Xiao-Chen Liu: Methodology, Software, Investigation, Formal analysis, Writing - original draft. **Jacob J.K. Kirkensgaard:** Software, Methodology, Resources. **Leif H. Skibsted:** Conceptualization, Methodology, Writing - review & editing, Supervision, Project administration, Funding acquisition.

Declaration of Competing Interest

The authors declare that they have no known competing financial interests or personal relationships that could have appeared to influence the work reported in this paper.

Acknowledgments

The authors acknowledge the support from China Scholarship Council (CSC) and from the Innovation Fund Denmark/FAPESP project – Novel Aging – Technologies and solutions to manufacture novel dairy products for healthy aging.

Appendix A. Supplementary material

Supplementary data to this article can be found online at https://doi.org/10.1016/j.foodres.2020.109867.

References

Bailey, A. L., Nehmer, W. L., & Elmore, R. O. (2010). U.S. Patent No. 7,781,003. Washington, DC: U.S. Patent and Trademark Office.

Bates, R. G., & Pinching, G. D. (1949). Resolution of the dissociation constants of citric acid at 0 to 50°, and determination of certain related thermodynamic functions. *Journal of the American Chemical Society, 71*(4), 1274–1283. https://doi.org/10.1021/ja01172a039.

Casey, W. H. (1988). Entropy production and the Ostwald step rule. *Journal of Physical Chemistry, 92*(1), 226–227. https://doi.org/10.1021/j100312a048.

Chattejee, K. P., & Dhar, N. R. (1924). Studies of sparingly soluble salts. *Journal of Physical Chemistry, 28*(10), 1009–1028. https://doi.org/10.1021/j150244a001.

Cheng, H., Garcia, A. C., Tang, N., Danielsen, B. P., & Skibsted, L. H. (2018). Combinations of isocitrate and citrate enhance calcium salt solubility and supersaturation robustness. *International Dairy Journal, 85*, 225–236. https://doi.org/10.1016/j.idairyj.2018.06.009.

Chung, S. Y., Kim, Y. M., Kim, J. G., & Kim, Y. J. (2009). Multiphase transformation and Ostwald's rule of stages during crystallization of a metal phosphate. *Nature Physics, 5*(1), 68–73. https://doi.org/10.1038/NPHYS1148.

Davies, C. W. (1962). *Ion association*. London: Butterworth-Heinemann (Chapter 3).

Dutronc, T., Terazzi, E., Guénée, L., Buchwalder, K.-L., Spoerri, A., Emery, D., Mareda, J., Floquet, S., & Piguet, C. (2013). Enthalpy-entropy compensation combined with cohesive free-energy densities for tuning the melting temperatures of cyanobiphenyl derivatives. *Chemistry A European Journal, 19*(26), 8447–8456. https://doi.org/10.1002/chem.201300587.

Goss, S. L., Lemons, K. A., Kerstetter, J. E., & Bogner, R. H. (2007). Determination of calcium salt solubility with changes in pH and PCO2, simulating varying gastrointestinal environments. *Journal of Pharmacy and Pharmacology, 59*(11), 1485–1492. https://doi.org/10.1211/jpp.59.11.0004.

Griessen, R., Boelsma, C., Schreuders, H., Broedersz, C. P., Gremaud, R., & Dam, B. (2020). Single quality factor for enthalpy-entropy compensation, isoequilibrium and isokinetic relationships. *ChemPhysChem, 21*(15), 1632–1643. https://doi.org/10.1002/cphc.202000390.

Hagelstein, V., Gerhart, M., & Wagner, K. G. (2018). Tricalcium citrate – A new brittle tableting excipient for direct compression and dry granulation with enormous hardness yield. *Drug Development and Industrial Pharmacy, 44*(10), 1631–1641. https://doi.org/10.1080/03639045.2018.1483389.

Hanzlik, R. P., Fowler, S. C., & Fisher, D. H. (2005). Relative bioavailability of calcium from calcium formate, calcium citrate, and calcium carbonate. *Journal of Pharmacology and Experimental Therapeutics, 313*(3), 1217–1222. https://doi.org/10.1124/jpet.104.081893.

Harris, D. C. (2007). *Quantitative chemical analysis* (7th ed.). New York: Craig Bleyer (Chapter 11).

Hartley, A., Paternoster, L., Evans, D. M., Fraser, W. D., Tang, J., Lawlor, D. A., Tobias, J. H., & Gregson, C. L. (2020). Metabolomics analysis in adults with high bone mass identifies a relationship between bone resorption and circulating citrate which replicates in the general population. *Clinical Endocrinology, 92*(1), 29–37. https://doi.org/10.1111/cen.14119.

Herdtweck, E., Kornprobst, T., Sieber, R., Straver, L., & Plank, J. (2011). Crystal structure, synthesis, and properties of tri-calcium di-citrate tetra-hydrate [Ca3(C6H5O7)2(H2O)2]·2H2O. *Zeitschrift fur Anorganische und Allgemeine Chemie, 637*(6), 655–659. https://doi.org/10.1002/zaac.201100088.

Holt, C., Lenton, S., Nylander, T., Sørensen, E. S., & Teixeira, S. C. M. (2014). Mineralisation of soft and hard tissues and the stability of biofluids. *Journal of Structural Biology, 185*(3), 383–396. https://doi.org/10.1016/j.jsb:2013.11.009.

Kaduk, J. A. (2018). Crystal structures of tricalcium citrates. *Powder Diffraction, 33*(2), 98–107. https://doi.org/10.1017/S0885715618000283.

Mansour, S. A. A. (1994). Thermal decomposition of calcium citrate tetrahydrate. *Thermochimica Acta, 233*(2), 243–256. https://doi.org/10.1016/0040-6031(94)85118-2.

Pak, C. Y., Harvey, J. A., & Hsu, M. C. (1987). Enhanced calcium bioavailability from a solubilized form of calcium citrate. *The Journal of Clinical Endocrinology & Metabolism, 65*(4), 801–805. https://doi.org/10.1210/jcem-65-4-801.

Palermo, A., Naciu, A. M., Tabacco, G., Manfrini, S., Trimboli, P., Vescini, F., & Falchetti, A. (2019). Calcium citrate: From biochemistry and physiology to clinical applications. *Reviews in Endocrine and Metabolic Disorders, 20*(3), 353–364. https://doi.org/10.1007/s11154-019-09520-0.

Rodrigo, M. M., Ribeiro, A. C., Verissimo, L. M., Esteso, M. A., & Leaist, D. G. (2019). Coupled diffusion in aqueous citric acid+ calcium citrate solutions. *The Journal of Chemical Thermodynamics, 131*, 314–321. https://doi.org/10.1016/j.jct.2018.11.003.

Sakhaee, K., & Pak, C. (2013). Superior calcium bioavailability of effervescent potassium calcium citrate over tablet formulation of calcium citrate after Roux-en-Y gastric bypass. *Surgery for Obesity and Related Diseases, 9*(5), 743–748. https://doi.org/10.1016/j.soard.2011.11.011.

Schmelzer, J. W., & Abyzov, A. S. (2017). How do crystals nucleate and grow: Ostwald's rule of stages and beyond. In *Thermal physics and thermal analysis* (pp. 195–211). Cham: Springer.

Skibsted, L. H. (2016). Mineral nutrient interaction: Improving bioavailability of calcium and iron. *Food Science and Biotechnology, 25*(5), 1233–1241. https://doi.org/10.1007/s10068-016-0196-2.

Threlfall, T. (2003). Structural and thermodynamic explanations of Ostwald's rule. *Organic Process Research & Development, 7*(6), 1017–1027. https://doi.org/10.1021/op030026l.

Tondapu, P., Provost, D., Adams-Huet, B., Sims, T., Chang, C., & Sakhaee, K. (2009). Comparison of the absorption of calcium carbonate and calcium citrate after roux-en-Y gastric bypass. *Obesity Surgery, 19*(9), 1256–1261. https://doi.org/10.1007/s11695-009-9850-6.

Van Santen, R. A. (1984). The Ostwald step rule. *Journal of Physical Chemistry, 88*(24), 5768–5769. https://doi.org/10.1021/j150668a002.

Vavrusova, M., Danielsen, B. P., Garcia, A. C., & Skibsted, L. H. (2018). Codissolution of calcium hydrogenphosphate and sodium hydrogencitrate in water. Spontaneous supersaturation of calcium citrate increasing calcium bioavailability. *Journal of Food and Drug Analysis, 26*(1), 330–336. https://doi.org/10.1016/j.jfda.2017.05.003.

Vavrusova, M., Garcia, A. C., Danielsen, B. P., & Skibsted, L. H. (2017). Spontaneous supersaturation of calcium citrate from simultaneous isothermal dissolution of sodium citrate and sparingly soluble calcium hydroxycarboxylates in water. *RSC Advances, 7*(6), 3078–3088. https://doi.org/10.1039/C6RA25807G.

Vavrusova, M., & Skibsted, L. H. (2016). Aqueous solubility of calcium citrate and interconversion between the tetrahydrate and the hexahydrate as a balance between endothermic dissolution and exothermic complex formation. *International Dairy Journal, 57*, 20–28. https://doi.org/10.1016/j.idairyj.2016.02.033.

Wang, L.-M., Wang, W., Li, X.-C., Peng, L., Lin, Z.-Q., & Xü, H.-Z. (2012). Calcium citrate: A new biomaterial that can enhance bone formation in situ. *Chinese Journal of Traumatology, 15*(5), 291–296. https://doi.org/10.3760/cma.j.issn.1008-1275.2012.05.007.